Detection of particles on the insulator surface in gas insulated DC systems

Maria Hering[1], Joachim Speck[1], Steffen Großmann[1], Uwe Riechert[2], Stefan Neuhold[3]

[1]Institut für Elektrische Energieversorgung und Hochspannungstechnik, TU Dresden
[2]High Voltage Products, ABB Schweiz AG, Zürich
[3]FKH Fachkommission für Hochspannungsfragen, Zürich

Summary

Due to the increasing need of space saving installations, the application of compact gas insulated systems is required. In spite of high quality standards during manufacturing and assembly, metallic particles cannot be excluded completely and turn out to be a critical defect in the typical nearly uniform electrical fields when decreasing the system's insulation strength. Charge carriers, produced at particle tips, influence the charging of insulating materials and thus the flashover behaviour of epoxy resin spacers, especially under DC voltage stress. Therefore, those defects have to be discovered during commissioning. Since efficient diagnostics require a metrological detectability of the defects, the paper describes the challenges of detection, using the behaviour of sticking particles on the insulator surface in gas insulated DC systems.

1 Introduction

Satisfying the requirements of recent energy transmission, like space saving installations, bridging vast distances between generation and consumption of energy as well as linking offshore wind farms, DC operated gas insulated systems are shifted into the focus.

Although experiences have been gained with many SF_6 gas insulated switchgears (GIS) and lines that have been in service under AC voltage since the 1960s, using direct current is challenging. Operating experiences of GIS under DC voltage have been existing from the ± 250 kV Kii Channel HVDC Link in Japan [1] since year 2000.

Since the distribution of the electrical field under DC stress is controlled by the temperature-dependent conductivities of the insulating materials, field inversion can be observed during capacitive-resistive transition [17]. Additionally, the accumulation of space and surface charges under DC stress has to be investigated, since it is influencing the insulation performance of gas insulated systems. These charge carriers can be produced by discharges due to several defects in GIS, especially by conducting particles.

1.1 Types of defects

Typical defects in GIS are comprehensively described in several publications, e.g. [2], [3] and shall therefore only be named shortly: voids and cracks in insulating materials, floating electrodes, free moving particles, particles or protrusions on the high voltage conductor or the enclosure and particles on insulating materials.

Considering return of service experience analyses, roughly 50 % of the dielectric failures in service of 420 kV GIS are related to particles on the insulator surface, on the enclosure or on the high voltage conductor [1], [4]. Therefore, the understanding of the failures and the measures to prevent them as well as the possibilities of their detection are essential. This paper examines the particles on the spacer surface.

1.2 Particles on spacer surface

"As GIS are hermetically sealed from the environment, the insulation reliability is very high. In spite of the high quality during manufacturing and assembly of the GIS with respect to the cleanliness, the occurrence of particles cannot be excluded." [5] Due to the electrostatic force under an applied voltage, metallic particles lift off and possibly adhere to the insulator surface. The need of detecting those failures is motivated by several phe-

nomenological investigations that state a strong decrease of the insulation strength.

"According to the literature, the behaviour of moving particles in general was comprehensively investigated at various voltage types (AC, DC, impulse voltage) [6], [7], [8], [9].

In comparison to free moving particles, the focus with particles, sticking on insulator surfaces, is set to AC and impulse voltage stress to define the dielectric dimensioning values and to detect possible particles in systems under operation. In [10] and [11], a stronger decrease of the insulation strength under lightning impulse (LI) voltage stress in comparison to AC voltage stress was stated, when a particle was adhered at the insulator surface. Also in [12] it was found, that the AC and LI breakdown voltage decrease with increasing length of the sticking particle.

The influence of a particle at spacer surface with electrode contact on the flashover behaviour was investigated in [13] under AC voltage and in [15] under very fast transient overvoltages.

Studies with particles on the insulator surface, which are not connected to one of the electrodes, are very rare with respect to an applied DC voltage." [5] Additionally to the lack of knowledge about the phenomenological behaviour of particles on the insulator surface under DC stress, the effect of space charge accumulation is decisive: duration and magnitude of the capacitive-resistive transition [17] can be influenced significantly.

Generally, it is known, that roughly 60 % of the dielectric failures could have been found by appropriate diagnostic techniques [1], [16]. But efficient diagnostics require a metrological detectability of the defects. The critical size of particles on insulating materials is stated around 2 mm [16] with an apparent charge according IEC 60270 of only 0.5 pC. The sensitivity of on-site tests depends strongly on the applied method. Using minimal requirement equipment resulting in a sensitivity of > 5 pC, it is quite challenging to detect this kind of defect.

2 Test setup

2.1 High voltage test circuit

In order to investigate flashover behaviour of insulators with adhesive particles, the following high voltage test circuit was utilised (*Figure 1*):
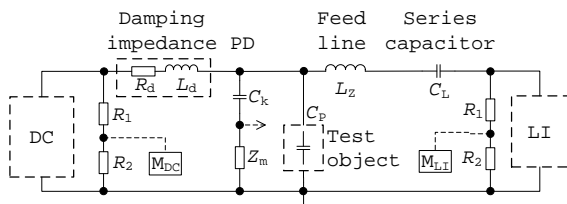

Figure 1: High-voltage test circuit

A three-stage Greinacher cascade is providing a high direct current voltage (DC). The lightning impulse voltage (LI) is created by a Marx generator. Since a breakdown in SF_6 causes very fast

transients, a damping impedance is protecting the DC cascade. It can also be used as a filter for PD measurements (IE 60270).

Both voltage stresses can be applied separately. Using a series capacitor, the superposition of DC and LI is possible. It has to be distinguished between unipolar and bipolar stress (*Figure 2*).
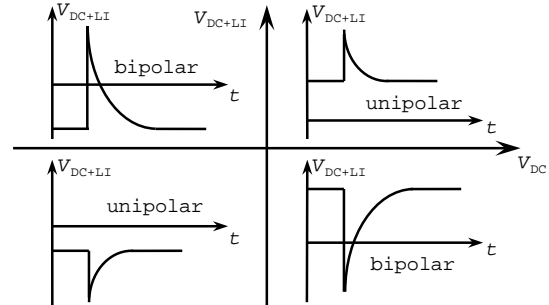

Figure 2: Superimposed voltage of DC and LI

2.2 Test chamber and specimen

Enclosure and high voltage part of the test chamber are standard GIS components (*Figure 3*). Cylindrical, epoxy resin test specimens were utilised to investigate the flashover behaviour of the quasi-homogeneous arrangement (*Figure 4*). Special designed electrodes guarantee the required field strength at the electrode surface and the interface between the epoxy resin insulator and SF_6.

Metallic particles were cut from an aluminium wire with a diameter of 0.8 mm to lengths between one and eight millimetres. They were fixed on the insulator with silicone adhesive at various positions along the surface. The absolute gas pressure was varied (0.1 … 0.5) MPa.

Since the test chamber is equipped with a gauge glass, it is possible to observe the PD and flashover behaviour with a camera. With an internal UHF sensor, sensitive PD detection is applicable.
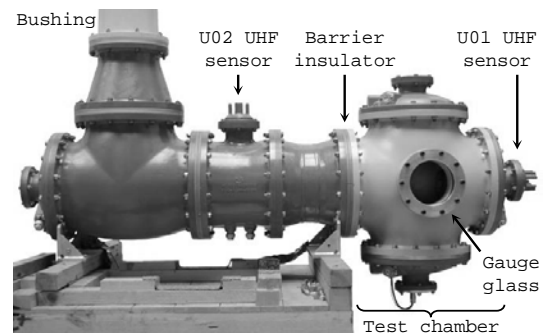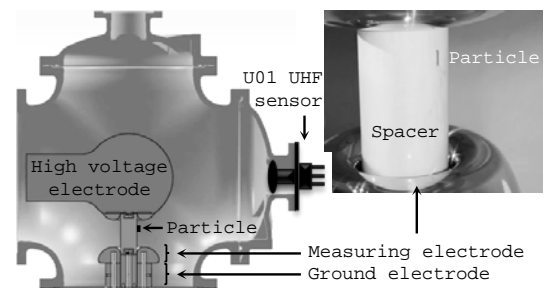

Figure 3: Test setup with test chamber

Figure 4: Test chamber with test specimen

3 PD detection methods

In the following, all applied PD detection methods are described shortly. During the investigations the optical observation, the PD current measurement and one of the typically used IEC method or UHF method were applied in parallel.

3.1 Optical detection

Using the gauge glass in the test chamber, the discharge behaviour of the particle can be observed with a system camera (ISO 6400, shutter speed 0.5 s). The image data is transmitted live via optical fibre to a monitor outside the test stand. To electromagnetically protect the camera, it is placed in a Faraday cage.

3.2 PD current measurement

As soon as the applied voltage is exceeding the inception voltage at the particle tips, partial discharges cause a measurable current. Therefore, the upper part of the ground electrode is insulated (*Figure 4*) and measures explicitly the current in the gas and not over the insulator surface. Expecting a direct current, the signal of the measuring electrode V_M is amplified and filtered, so that only low-frequency signal components are received by the logger. Using Bluetooth wireless transmission, the signals can be sent to a computer during the ongoing measurement to correlate them with the measured applied DC voltage (*Figure 5*). The measuring shunt R_M can be switched between 10 kΩ and 100 kΩ, depending on the expected current.

Due to the parallel observation with the camera, it can be confirmed, that an abrupt rise of the current signal is correlated to the inception of the PD at the particle tips.
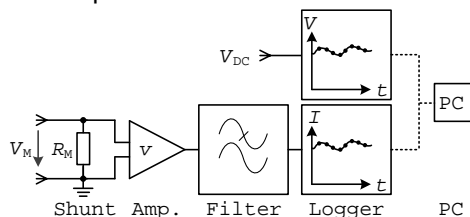

Figure 5: Principle of measuring the PD current of the particle on the insulator surface

3.3 Conventional method (IEC 60270)

The conventional PD detection method was applied according to IEC 60270 [14] with the test object grounded and the measuring impedance Z_m in series with the coupling capacitor C_k. The damping impedance was used as a filter, suppressing the noise from the voltage source and blocking the PD pulses from flowing through the DC generator. Due to other apparatuses in the lab, the noise was not lower than 3 pC. In order to distinguish between internal PD from the particle and disturbances caused by the AC supply at these high voltages, the phase relation of the transformer, which is feeding the DC cascade, was provided to the PD measurement system.

3.4 UHF method

Applying the UHF method with a bandwidth range of 300 MHz to 3 GHz to detect PD has two main reasons [19]: First of all, external disturbances, mainly in the low-frequency range, are widely spread and secondly, PD pulses in SF_6 are well-known for their frequency content of up to 15 GHz [18]. Since two UHF sensors (U01 and U02 as internal sensors, see *Figure 3*) are installed in the test setup, a sensitivity check can be performed [19], [20]. Using a spectrum analyser in full span mode (frequency domain) and zero span mode (time domain), the UHF signal is displayed. The full span mode is using a bandwidth range of 100 MHz to 1.8 GHz. In order to analyse the signals in the time domain, zero span mode is applied at a certain centre frequency with a sweep time of 34 ms and a resolution bandwidth of 3 MHz. Additionally, the down converted signals of the zero span mode are sent to an oscilloscope.

4 Influence of the adhesive particle on the dielectric insulation performance

Investigating the particle's behaviour, several parameters were varied. Their significance for the dielectric insulation performance will be described below. In order to determine the flashover voltage the experiments were carried out as a slow voltage rising test with approximately 5 kV/s under both positive and negative DC stress.

4.1 Influence of particle length

Using the PD current measurement and the optical monitoring system, the inception voltage is determined by an abrupt current rise or a visible glowing at the particle tips.
Figure 6 shows the measured inception and flashover voltage at 0.1 MPa SF_6 with particle lengths up to 8 mm. The longer the particle is, the lower the flashover voltage. But even quite long particles of 8 mm length are only reducing the insulation performance by 17 %. This can be explained as follows: Even at 50 % of the breakdown voltage without a particle, partial discharges occur at the particle tips.
Due to the corona stabilisation effect, the space charges at the particle tips are weakening the strong electrical field [21], [22]. Hence, a higher voltage is needed to initiate the flashover.

4.2 Influence of particle position

As described in [5], there is a strong dependence from the flashover voltage on the particle position and a possible contact to the electrode. It can be seen in *Figure 7*, that a particle in the middle of the insulator results in the same decrease of the flashover voltage (ca. 12 %) for both polarities.

The strongest decrease can be found in position A^a for positive and in position D for negative polarity. The electrical field strength is higher at the particle tip with a shorter distance to the electrode. Hence, the discharges partly bridge the gap. As known from [21], the breakdown voltage of a disturbed quasi-homogeneous electrical field is lower under positive DC stress. This is comparable with the particle near the positive electrode, thereby confirming the lower flashover voltage.
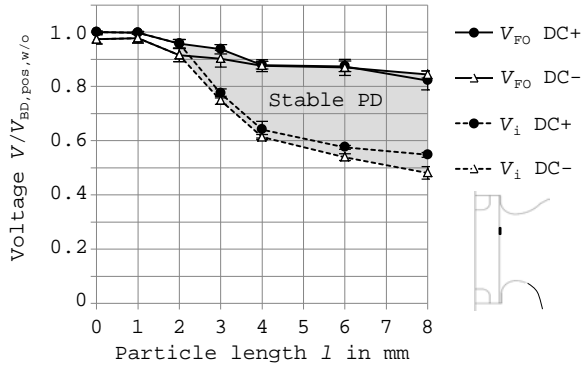

Figure 6: Flashover voltage V_{FO} and inception voltage V_i of the insulator with particles of different lengths related to the flashover voltage without a particle at 0.1 MPa
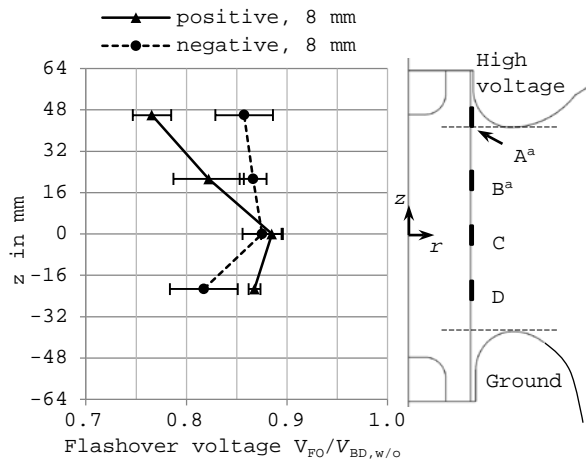

Figure 7: Flashover voltage V_{FO} of the insulator with an 8 mm particle at different positions related to the breakdown voltage without a particle $V_{BD,w/o}$ at 0.1 MPa
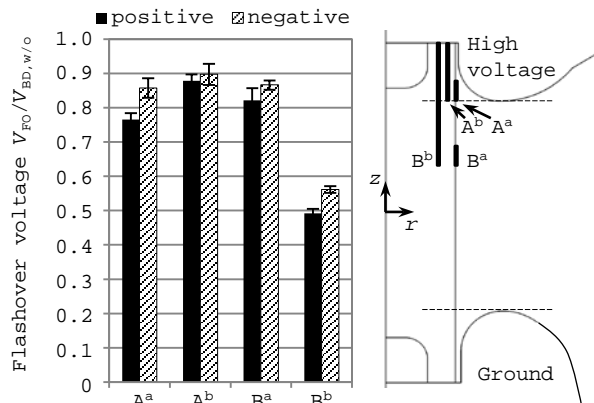

Figure 8: Flashover voltage V_{FO} of the insulator with particles in different positions related to the breakdown voltage without a particle $V_{BD,w/o}$ at 0.1 MPa

Since the particle on the insulator surface has a floating potential, space charges of both polarities occur at the particle tips. Therefore, it is necessary to investigate the influence of a particle with and without electrode contact [5]. *Figure 8* shows the comparison of two different positions A and B.

"Since the electrical field strength at the particle tips in position A^b with electrode contact is higher than in A^a without electrode contact, partial discharge occurs at a lower voltage level. The more stable space charge at the tip leads to a higher flashover voltage with electrode contact (A^b) than without (A^a). The difference in the flashover voltages of positions B^a and B^b is significant. Particles in B^b with contact to the high voltage electrode reduce the flashover distance clearly. Flashover occurs at 55 % of the breakdown voltage level without a particle. The influence of the particle without contact to the high voltage electrode (B^a) is comparable to A^a and A^b." [5]

4.3 Influence of gas pressure

As stated, stable space charges occur at the particle tips at a gas pressure of 0.1 MPa and prevent a strong decrease of the flashover voltage.

The following investigations were performed with an 8 mm long particle in position B^a under both positive and negative DC and LI voltage stress up to a pressure of 0.5 MPa (*Figure 9*).

The inception voltage V_i is increasing with an increasing gas pressure up to 0.3 MPa. At higher pressures, discharges before the flashover have never been observed, neither with camera system nor with a measured PD current. Thus, the inception voltage equals the flashover voltage.

The flashover voltage is almost proportionally increasing with the gas pressure up to 0.2 MPa. Due to the limits of the DC cascade, the flashover voltage at 0.2 MPa and 0.25 MPa could not have been determined. The maximal flashover voltage has to be expected in this pressure range.
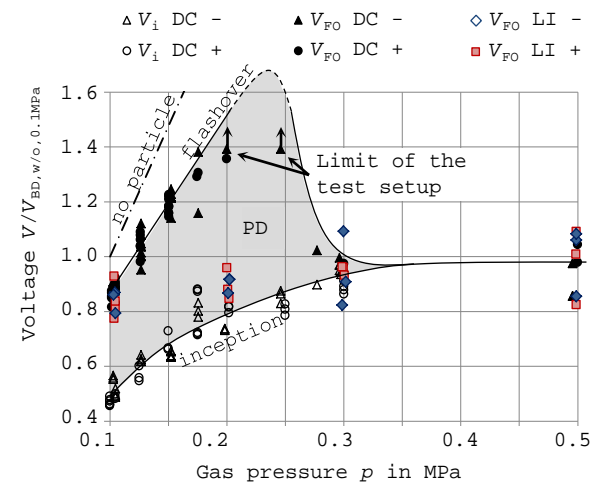

Figure 9: Flashover voltage V_{FO} and inception voltage V_i of the insulator with an 8 mm particle related to the flashover voltage without a particle at 0.1 MPa in dependence on the gas pressure

If the gas pressure exceeds 0.275 MPa, the flashover voltage will be significant low and comparable to values at 0.125 MPa. Even with higher pressures up to 0.5 MPa, the flashover voltage is not increasing, because the corona stabilisation is no longer working. Due to the high pressure the glow charge is becoming unstable or rather not occurring at pressures > 0.3 MPa.

In order to confirm the effect of the corona stabilisation, the flashover behaviour was investigated under LI voltage stress. Since lightning impulse voltage is rising rapidly, glow discharges are not being built up. With the missing stabilisation effect, the LI and DC flashover voltage at 0.5 MPa equals that at 0.125 MPa.

4.4 Effect of superimposed voltages

Investigations with DC voltage stress show, that the corona stabilisation is playing a key role when an adhesive particle is present on the insulator surface. If it is missing, like under LI voltage stress, the system's insulation strength will be severely reduced.

Considering experimental investigations with superimposed voltage stress of DC and LI, it was expected that the corona discharge of the applied DC voltage helps to prevent a strong decrease of the insulation strength due to LI voltage.

Figure 10 shows the flashover voltage under DC stress superimposed with LI: unipolar and bipolar. First of all, it can be seen, that the decrease with particle under pure LI voltage (ordinate) is greater due to the missing corona discharges than under pure DC voltage (diagonal). The superimposed tests were carried out at DC voltage levels with and without glow discharges before applying the impulse voltage, in order to investigate the influence of the corona stabilisation.

The results do not depict a dependency on whether discharges are occurring or not. Alone the applied DC voltage shows a distinct effect on the flashover voltage. It can be clearly distinguished between unipolar and bipolar behaviour.

In case of positive LI, a negative space charge possibly starts at the particle tip close to the high voltage electrode. The space charges then move to the positive high voltage electrode. Dependent on the impulse duration, they accumulate as surface charges as soon as the necessary electrostatic force of the electrical field is too low. If LI is superimposed to DC, the electrostatic force will constantly change the field relations. Furthermore, it has to be mentioned, that the flashover voltage was gained by a voltage rising test with LI. As stated in [10], the previous impulses influence the flashover voltage as well.

Considering the unipolar superposition, an influence of the DC voltage on the superimposed flashover voltage can hardly be noticed. Contrarily, the bipolar behaviour is different. The higher the DC voltage is, the higher the necessary LI voltage to initiate a flashover, but the lower the superimposed flashover voltage. As *Figure 2* shows, the bipolar sum of DC and LI voltage has the opposite polarity of the applied DC voltage. The flashover occurs due to the field inversion.
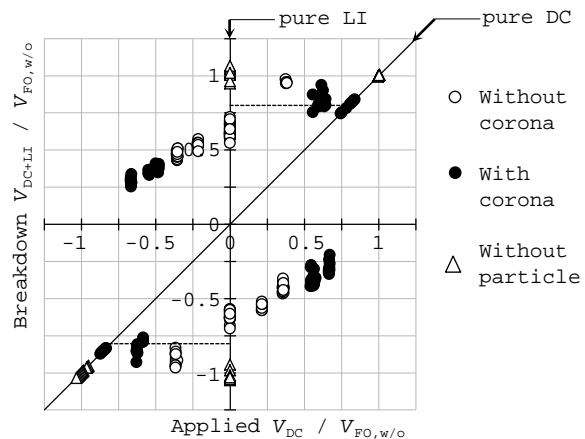

Figure 10: Superimposed flashover voltage (DC and LI) dependent on the applied DC voltage at 0.1 MPa for an 8 mm long particle, related to the flashover voltage without a particle

5 Detection of the adhesive particle

For the investigations of different detection methods, an 8 mm long particle was utilised. The particle was placed in a position, where the normal component of the undisturbed electrical field along the insulator surface is zero [5].

5.1 Optical detection

As soon as the applied voltage exceeds the inception voltage, glow discharges at the particle tips can be observed (*Figure 11*). The higher the voltage is, the brighter and more expanded the discharges. With particles smaller than 3 mm, no discharges can be seen before breakdown, which was also proved by the PD current measurement. The breakdown voltage has hardly decreased.

At higher gas pressures (> 0.275 MPa), the spherical discharges get constricted and small streamers start at the tips. With this, the discharges lose their visible stability and are extinguished and ignited repetitively. The breakdown occurs after few minutes out of the instable discharge. At a pressure of 0.5 MPa, no visible partial discharges occur before breakdown.
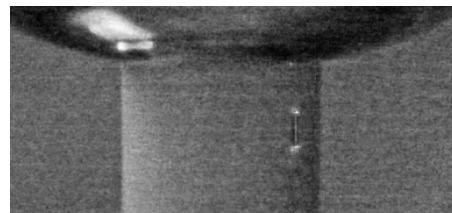

Figure 11: Partial discharges at the particle tips

5.2 Detection by PD current

Since both the camera system and the current measurement work during the ongoing investigation, a good correlation could be found. As soon as

an abrupt current rise occurs, the particle tips glow. The higher the applied voltage, the higher is the measured current (*Figure 12*). Due to the low pass character of the measuring electrode, high-frequency discharges cannot be detected sufficiently. Thus, the current provides information about intensity and stability of the discharge.

As known from the observation with the camera, the discharges are getting unstable at pressures higher 0.275 MPa. *Figure 13* shows a lower current at 0.3 MPa in comparison to 0.1 MPa, since the measuring electrode is not registering the high-frequency components of the unstable discharge.
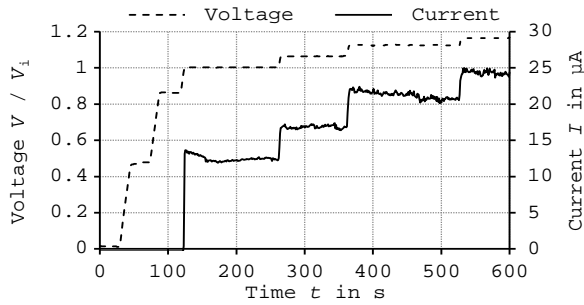
Figure 12: PD current and applied voltage. Gas pressure 0.1 MPa, particle length 8 mm
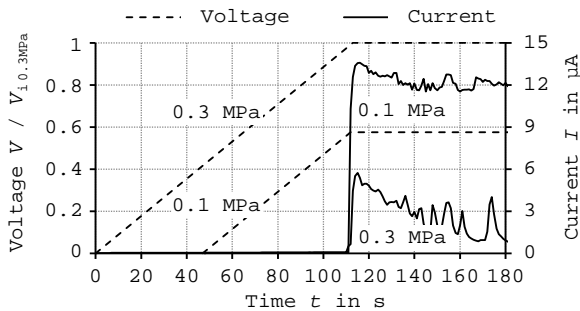
Figure 13: PD current during voltage rising till PD inception at 0.1 MPa and 0.3 MPa

5.3   Conventional PD Detection

Particles in GIS under AC voltage stress produce typical PD signals. The measured apparent charge of the discharges is sufficiently higher than the noise level when the inception voltage of the particle tips is exceeded (*Figure 14*, top). Due to the close insulating surface, the pattern is shifted by more than 60 degrees in comparison to a protrusion connected to the electrodes without an insulator [15].

Applying DC voltage, the missing phase relation is one of the biggest challenges when identifying defects. *Figure 14* (middle) shows, that the measured apparent charge will hardly change, no matter if the particle produces PD (right) or not (left).

At higher gas pressures around 0.3 MPa, the discharges are getting visibly unstable and are extinguished and ignited repetitively. In this case, the measured apparent charge is significantly higher as soon as the inception voltage of the particle tips is exceeded (*Figure 14*, bottom).

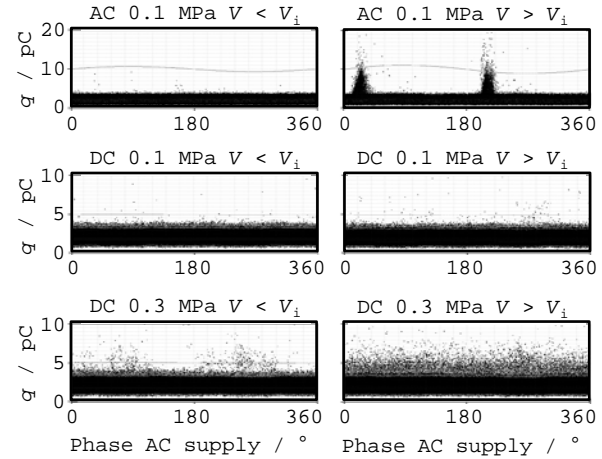However, the magnitude is still very close to the noise level.

Figure 14: Measured apparent charge without (left) and with PD (right) at the particle under AC and DC stress. Pressure: 0.1 MPa and 0.3 MPa

5.4   Detection by UHF method

First, the frequency spectrum between 100 MHz and 1.8 GHz without an active PD source was recorded (*Figure 15*). The lower line is a single frequency sweep and shows the constantly emitted noise, like television and mobile communication signals. The upper line is given by holding the maximum amplitude of all the frequencies and also recognises rarely occurring signals.

Exceeding the applied voltage over the inception voltage of the particle tips, the frequency spectrum changes (*Figure 16*) due to the partial discharges at the particle. Zero span mode was applied at 270 MHz, 690 MHz and 1.333 GHz (*Figure 17*).
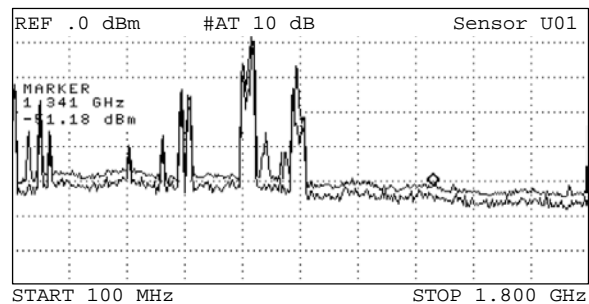
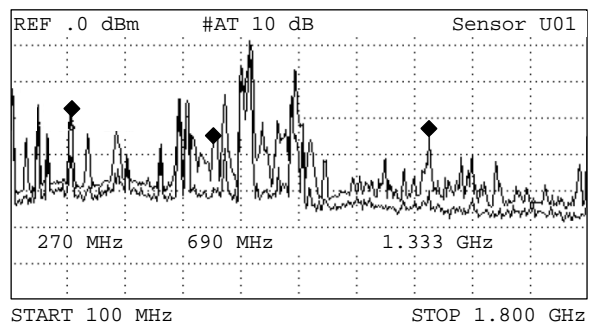*Figure 15: Frequency spectrum of sensor U01 with no active PD source at a voltage $V \ll V_i$*

Figure 16: Frequency spectrum of sensor U01 with active PD source (particle on insulator) at $V \gg V_i$
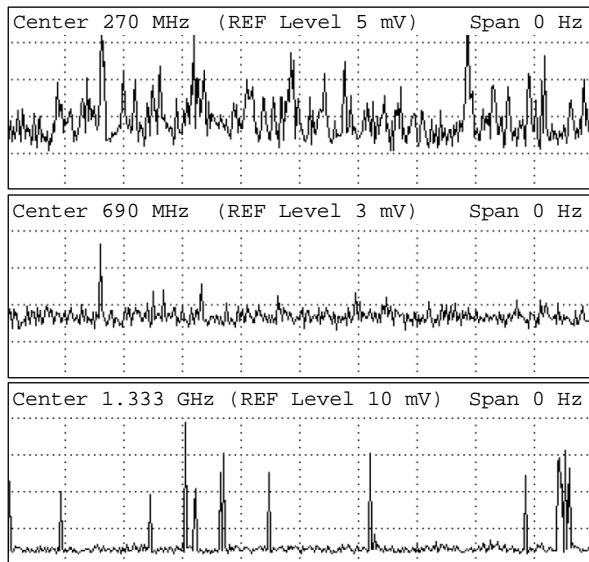
```
Center 270 MHz   (REF Level 5 mV)      Span 0 Hz
```

```
Center 690 MHz   (REF Level 3 mV)      Span 0 Hz
```

```
Center 1.333 GHz (REF Level 10 mV)     Span 0 Hz
```

Figure 17: Zero span with active PD source at a voltage V >> Vᵢ at different center frequencies with a resolution bandwidth of 3 MHz and a sweep time of 34 ms
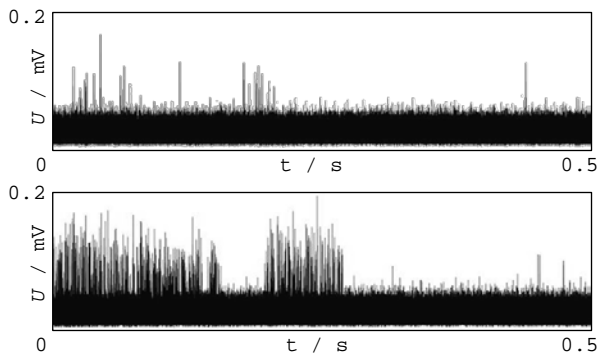

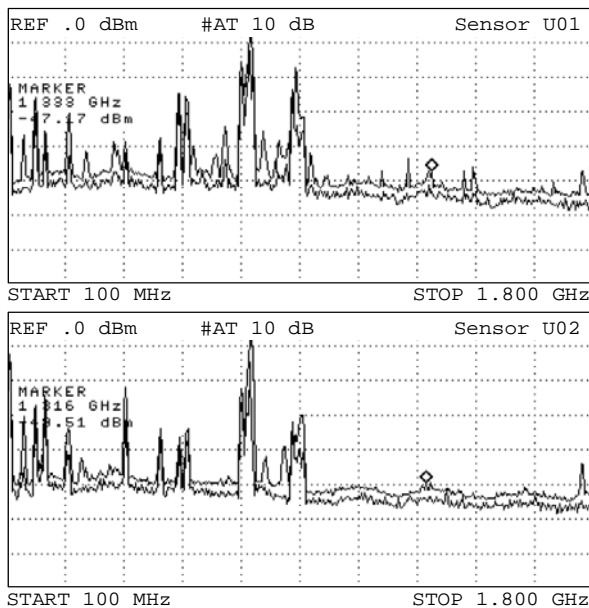*Figure 18: PD signal of sensor U01 at the oscilloscope at 1.333 GHz*

Figure 19: Frequency spectrum of sensors U01 (top) and U02 (bottom) with active PD source (particle on insulator) at a voltage V >> Vᵢ

Figure 18 shows the PD signal at the oscilloscope at 1.333 GHz twice within half a second. Patterns or regularities are much more difficult to discover compared to PD signals at AC voltage. They can be subject to future research. The signal changes rapidly and randomly not only within seconds, but also within minutes, what can be seen when comparing *Figure 16* and *Figure 19* (top) with 30 minutes in between.

Although the UHF sensor U01 is mounted in the same compartment as the PD source, the received signal is relatively weak. *Figure 19* compares the signals of the sensors U01 and U02.

6   Conclusions

Under DC voltage stress and at low SF_6 pressures < 0.2 MPa, corona stabilisation plays a key role for the flashover behaviour, because even a quite long particle on the insulator surface only reduces the flashover voltage by 17 %. In contrast, the decrease under LI was about 40 % due to missing glow discharges at the particle tips.

Intensity and stability of the corona discharges are strongly dependent on the gas pressure. The maximal flashover voltage was reached at pressures around (0.2…0.25) MPa. High pressures impede a stable glow discharge, so that from 0.3 MPa flashover occurs without measureable previous partial discharges. Since the insulation strength of the system with particle on the insulation at 0.5 MPa equals that at 0.125 MPa, the necessity of detecting these defects is evident.

Measuring the PD current is very robust and detecting the particle reliably, but is not suitable for the practical use during onsite measurements. Since charge carriers move along the electrical field lines, the PD current is strongly dependent on the measuring electrode position and therefore not applicable onsite.

Using the conventional method according to IEC 60270, particles on insulating surfaces are difficult to detect, which is also confirmed in [20] and [23]. Especially with very stable glow discharges at the particle tips, the application of this impulse-based method is challenging. In contrast, however, the UHF method seems to be more promising.

Applying the UHF method to investigate a fixed particle on the insulator, it can at least be found by analysing the frequency spectrum. Although all external conditions seem to be constant, the signal changes randomly not only within seconds, but also within several minutes, see [23]. In the typical practical case of not knowing, if there is a defect and which kind of defect it is, a reliable detection of particles on the insulator surface is challenging. It is well-known that barrier insulators are damping the signal. Nevertheless, even with an UHF sensor and a PD source on the insulator surface in the same compartment, the signal amplitude is low.

Using LI voltage stress, the particle can be found quite reliably, also stated in [9], [10]. But in this case, the damage due to a flashover is quite high. One alternative could be the use of AC voltage stress during commissioning. Since the discharges at the particle tips reignite every half wave, the detectability is given (see *Figure 14*). Phase resolved PD patterns allow defect identification. Furthermore, lower pressures offer the detection with less flashover risk. This approach is also applicable for fixed particles on conductor and enclosure. Considering superimposed voltage (DC+LI), corona discharge due to the DC voltage has no influence on the insulation strength. The flashover voltage is strongly dependent on the value of the applied DC voltage. With unipolar stress, the superimposed flashover voltage is similar to that with pure DC. With bipolar stress, the superimposed flashover voltage gets lower with a higher DC voltage. Just considering the superimposed voltage is misleading with regard to the actual dominating field strength. In this case, the field strength cannot be derived from the voltage level due to the occurring space charges under DC voltage stress. During unipolar stress, already low impulse amplitudes lead to breakdown, whereas bipolar stress needs high LI amplitudes, although the flashover voltage is rather low.

References

[1] M. Hirose, S. Hara and Y. Makino: Outline of the Kii channel HVDC link. Power Engineering Society Summer Meeting, vol. 1, pp. 349-362, 2001.

[2] CIGRÉ Working Group D1.28: Optimized gas-insulated systems by advanced insulation techniques. Technical Brochure No. 571, April 2014.

[3] S. Neuhold: On-site tests of GIS. Highvolt Kolloquium, Dresden, 2011.

[4] C. Neumann: PD measurement on GIS of different design by non-conventional UHF sensors. CIGRÉ Session, Paris, 2000.

[5] M. Hering, J. Speck, S. Großmann, U. Riechert: Investigation of particles on insulator surfaces in gas insulated systems under DC stress. CEIDP, Des Moines 2014.

[6] C. Cooke, R. Wootton and A. Cookson: Influence of particles on AC and DC electrical performance of gas insulated systems at extra-high voltage. IEEE Transactions on Power Apparatus and Systems, vol. 96, no. 3, pp. 768-777, May 1977.

[7] Westinghouse Research and Development Center: Investigation of High Voltage Particle-Initiated Breakdown in Gas Insulated Systems. EPRI Project 7835 Report, Pittsburgh, Pennsylvania, 1979.

[8] M. Holmberg, S. Gubanski: Motion of metallic particles in gas insulated systems. Electrical Insulation Magazine, IEEE, vol.14, no.4, 1998

[9] W. Mosch, W. Hauschild, J. Speck, S. Schierig: Phenomena in SF_6 insulations with particles and their technical valuation. ISH, Milan, 1979.

[10] R. Schurer: Der Einfluss von Störstellen auf Stützeroberflächen auf die elektrische Festigkeit von Isolieranordnungen in SF_6-isolierten Anlagen. PhD Thesis, Universität Stuttgart, 1999.

[11] A. Imano: Beeinflussung der elektrischen Festigkeit von N2/SF_6- und Luft/SF_6-Isolationen durch Metallpartikel auf der Stützeroberfläche. PhD Thesis, Uni Stuttgart, 2001.

[12] M. Hosokawa, F. Endo, T. Yamagiwa, T. Ishokawa: Particle-initiated breakdown characteristics and reliability improvement in SF_6 gas insulation. IEEE Transactions on Power Delivery, vol.1, no.1, pp.58-65, January 1986.

[13] N. Hayakawa, et al.: Dependence of partial discharge characteristics at spacer surface on particle size in SF_6 gas insulated system. CMD, Beijing, April 2008.

[14] DIN EN 60270:2001-08: Hochspannungs-Prüftechnik – Teilentladungsmessungen (IEC 60270:2000); Deutsche Fassung EN 60270:2001.

[15] S. Tenbohlen: Der Einfluss dielektrischer Oberflächen auf die Durchschlagsentwicklung in einer störstellenbehafteten SF_6-Anordnung. Dissertation, RWTH Aachen, 1997.

[16] CIGRÉ Joint Working Group 33/23.12: Insulation coordination of GIS; return of experience on site tests and diagnostic techniques. Electra no. 176, February 1998.

[17] M. Hering, R. Gremaud, J. Speck, S. Großmann, U. Riechert: Flashover behaviour of insulators with inhomogeneous temperature distribution in gas insulated systems under DC voltage stress. ICHVE, Poznan, 2014.

[18] A. Reid, M. Judd: Ultra-wide bandwidth measurement of partial discharge current pulses in SF_6. J. Phys. D. Appl. Phys., vol. 45, no. 16, April 2012.

[19] N. Kock, B. Coric, R. Pietsch: UHF PD detection in gas-insulated switchgear – suitability and sensitivity of the UHF method in comparison with the IEC method. IEEE Electrical Insulation Magazine, 1996.

[20] CIGRÉ, Joint Task Force 15/33/03.05: Partial Discharge Detection System for GIS: Sensitivity Verification for the UHF Method and the Acoustic Method. Electra, No. 183, April 1999, pp. 75 – 87.

[21] W. Mosch, W. Hauschild: Hochspannungsisolierungen mit Schwefelhexafluorid. Verlag Technik, Berlin 1979.

[22] T. Hinterholzer, W. Boeck: Breakdown in SF_6 influenced by corona-stabilization. CEIDP, Victoria 2000.

[23] R. Piccin: Partial Discharges Analysis in HVDC Gas Insulated Substations. PhD thesis, Delft University of Technology, 2013.

Zusammenfassung

Der Bedarf an platzsparenden Schaltanlagen erfordert den Einsatz kompakter, gasisolierter Systeme. Metallische Partikel – trotz hoher Qualitätsstandards bei Fertigung und Montage nicht völlig auszuschließen – erweisen sich in den typischerweise schwach inhomogenen Anordnungen als besonders kritische Feldstörung, da sie das Isolationsvermögen der Anlage herabsetzen. Gleichzeitig beeinflussen die an den Partikelspitzen produzierten Ladungsträger insbesondere bei Gleichspannungsbetrieb die Aufladung von Isolierstoffteilen und damit das Überschlagsverhalten der Feststoffisolatoren. Ziel während der Inbetriebnahme muss es deshalb sein, etwaige Partikel aufzufinden. Eine effektive Diagnostik setzt jedoch die messtechnische Detektierbarkeit derartiger Störstellen voraus. Die dabei auftretenden Herausforderungen werden anhand des Verhaltens fester Störstellen auf Isolierstoffoberflächen in Gleichspannungssystemen beschrieben.

Author

Dipl.-Ing. Maria Hering
Technische Universität Dresden
Institut für Elektrische Energieversorgung und Hochspannungstechnik
Mommsenstraße 10
01062 Dresden

maria.hering@tu-dresden.de